International Journal of Nanoelectronics and Materials
Volume 16, No. 4, October 2023 [771-782]

Electrochemiluminescence of Carbon Dots and Nitrogen-Doped Carbon Dots from a Microwave-Assisted Method

Nurul Izzati Akmal Mohd Azman[1], Muhammad Amirul Afiq Abdul Halim[1], Nur Syakimah Ismail[1, 2*], Nur Hamidah Abdul Halim[3], Nurjuliana Juhari[1, 2], Norhayati Sabani[1, 2], Siti Aisyah Shamsudin[4], Eiichi Tamiya[5]

[1]Faculty of Electronic Engineering & Technology, Universiti Malaysia Perlis (UniMAP), Perlis, Malaysia.
[2] Centre of Excellence Micro System Technology (MiCTEC), Universiti Malaysia Perlis (UniMAP), 02600 Arau, Perlis, Malaysia
[3]Institute of Nano Electronic Engineering (INEE), Universiti Malaysia Perlis (UniMAP), Perlis, Malaysia
[4]Department of Applied Physics, Faculty of Science and Technology, Universiti Kebangsaan Malaysia, 43600, Bangi, Selangor, Malaysia
[5]Advanced Photonics and Biosensing Open Innovation Laboratory, AIST-Osaka University, Osaka University, 2-1 Yamadaoka, Suita, Osaka, 565-0871, Japan

Received 24 September 2022, Revised 5 April 2023, Accepted 10 April 2023

ABSTRACT

This research focuses on the use of carbon dots (CDs) and nitrogen-doped carbon dots (NCDs) synthesized using a microwave-assisted method as electrochemiluminescence (ECL) luminophores. CDs have been synthesized using citric acid, while various concentrations of nitrogen-doped CDs have been successfully obtained by varying the amount of urea from 1 to 3 g with citric acid to produce NCD1, NCD,2 and NCD3. The ECL mechanism of CDs and NCDs on screen-printed electrodes has been studied using cyclic voltammetry (CV). ECL emission from as-prepared CDs and NCDs was observed in PBS with potassium persulfate ($K_2S_2O_8$) as a co-reactant. The addition of potassium chloride (KCl) as a supporting electrolyte displays fast electroreduction of CDs and $K_2S_2O_8$ to expedite the generation of CDs and peroxydisulfate radicals that simultaneously increase ECL intensity. Furthermore, as the concentration of nitrogen-doped CDs increases, so does the intensity of the ECL. NCD3 shows the highest ECL intensity by an increment of 86.4% in comparison to CDs in PBS with the addition of $K_2S_2O_8$ and KCl. Finally, optimization of ECL measurement was carried out in terms of CV potential range, concentration of luminophore, supporting electrolyte, and co-reactant using NCD3 luminophore. The CV potential range at 0 to -2 V shows 50 mV of early CV reverse onset potential that resulted in an increase of 52.9% ECL intensity. Meanwhile, 30x dilution of NCD3, 0.1 M of supporting electrolyte KCl, and 0.1 M of co-reactant $K_2S_2O_8$ show the optimum value to obtain high ECL intensity.

Keywords: Electrochemiluminescence, Carbon dots, Nitrogen-doped carbon dots, luminophore, co-reactant.

1. INTRODUCTION

The prospective applications of carbon dots (CDs) as a novel type of quantum dot in bioimaging, biosensors, catalysis, and drug delivery have garnered a lot of attention in recent years [1-4]. Compared to conventional inorganic quantum dots, CDs have a variety of advantages, including low toxicity, chemical inertness, biocompatibility, and the absence of photobleaching [5]. In general, CDs can be produced using both top-down and bottom-up methods. Top-down methods such as arc discharge, laser ablation, and electrochemical oxidation are used to break bigger crystalline carbon structures into smaller ones. Meanwhile, bottom-up methods like

---

[*] Corresponding author: syakimah@unimap.edu.my

hydrothermal, solvothermal, microwave-assisted, and thermal pyrolysis are used to create CDs from molecular precursors [6].

Previous studies have shown that the microwave-assisted approach has been more popular due to its simplicity in synthesis and economic viability [7]. Furthermore, this type of synthesis yields 10-30% CDs in a short reaction time with repeatable results. The hydrophilic carboxyl and hydroxyl groups that make up the CDs molecule provide them with water solubility and versatility properties. Many studies have focused on the CD fluorescence characteristics, surface passivation, and heteroatom doping such as nitrogen (N), sulphur (S), and phosphorus (P). Element doping is a more effective strategy than surface passivation since it may change CDs' inherent characteristics, such as improving certain electrical and optical properties and boosting the quantity of active sites on CD surfaces. It has been found that adding extra active sites by doping CDs with electron-rich nitrogen atoms can produce unique fluorescence phenomena and unexpected capabilities [8].

CDs feature unique color-tunable photoluminescence (PL) emission due to size, surface, and edge effects that are uncommon in graphene, fullerene, and carbon nanotubes. As a result, fluorescent CDs are expected to be ideal luminophore candidates for electrochemiluminescence (ECL) sensors. In general, the ECL process of CDs involves two pathways, namely annihilation and co-reactant [9-10]. The potential cycle enabled the CDs in the annihilation pathway to create their anion ($CD^{\bullet +}$) and cation ($CD^{\bullet -}$) radicals. The excited CD^* is created as a result of the electron-transfer annihilation of these two oppositely charged carriers ($CD^{\bullet +}$ and $CD^{\bullet -}$). Finally, the excited CD^* made a radiative transition back to the ground state by emitting a photon [11]. The ECL reaction mechanism for CDs through the annihilation pathway is stated as equations (1) to (4).

$$\mathrm{CD} - e^- \rightarrow \mathrm{CD}^{\cdot +} \tag{1}$$

$$\mathrm{CD} + e^- \rightarrow \mathrm{CD}^{\cdot -} \tag{2}$$

$$\mathrm{CD}^{\cdot +} + \mathrm{CD}^{\cdot -} \rightarrow \mathrm{CD}^* + \mathrm{CD} \tag{3}$$

$$\mathrm{CD}^* \rightarrow \mathrm{CD} + \hbar\nu \tag{4}$$

ECL using the co-reactant pathway is formed by one-directional potential scanning on an electrode in the presence of a luminophore CD and a heterogeneously introduced co-reactant that has strong solubility, stability, quick kinetics, electrochemical characteristics, and a low ECL background [10]. Studies have demonstrated that the ECL intensity of CDs using sulfite [12] or peroxydisulfate [13] co-reactants is greatly improved compared to the annihilation approach. In the co-reactant pathway, the electrochemical reduction of $S_2O_8^{2-}$ produces the strong oxidizing intermediate, $SO_4^{\bullet -}$. Reverse scanning also allows for the reduction of CDs to $CD^{\bullet -}$. After that, $CD^{\bullet -}$ and $SO_4^{\bullet -}$ could react to produce the excited states of CD^*, which decayed to the ground state while emitting light [14]. The ECL reaction mechanism for CDs with peroxydisulfate co-reactant is stated as equations (5) to (8) [15].

$$\mathrm{CD} + e^- \rightarrow \mathrm{CD}^{\cdot -} \tag{5}$$

$$\mathrm{S_2O_8}^{2-} + e^- \rightarrow \mathrm{SO_4}^{\cdot -} + \mathrm{SO_4}^{2-} \tag{6}$$

$$\mathrm{SO_4}^{\cdot -} + \mathrm{CD}^{\cdot -} \rightarrow \mathrm{CD}^* + \mathrm{SO_4}^{2-} \tag{7}$$

$$\mathrm{CD}^* \rightarrow \mathrm{CD} + \hbar\nu \tag{8}$$

According to Wang et al., the hydrothermal nitrogen doping of CDs can alter their electrical structure, resulting in a wider band gap and slower decay dynamics [15]. These two factors caused nonradiative recombination to decline and radiative recombination to increase, which significantly improved ECL performance. Herein, we investigate the ECL mechanism of CDs and NCDs that were produced using the microwave-assisted method. We also observed the effect of varying the urea amount during the synthesis process in order to produce various concentrations of nitrogen-doped CDs towards ECL intensity. Finally, we examined various factors that influence the ECL intensity of NCDs, such as cyclic voltammetry (CV) scan potential range and concentration of luminophore, co-reactant and supporting electrolyte.

2. EXPERIMENTAL

2.1 Material and Reagent

Citric acid ($C_6H_8O_7$), urea (CH_4N_2O), potassium persulfate ($K_2S_2O_8$) and potassium chloride (KCl) were obtained from HAMBURG Trading Corporation, Malaysia. Phosphate buffer solution (PBS, 0.1 M, pH 7.4) was prepared using potassium phosphate dibasic (K_2HPO_4) and potassium phosphate monobasic (KH_2PO_4). All the chemicals were used as received.

2.2 Synthesis of Carbon Dots and Nitrogen-doped Carbon Dots

Citric acid is a common precursor to produce CDs [16] and the addition of urea is proven to yield NCDs [17]. Table 1 shows the ratio of citric acid to urea in producing CDs and the various concentrations of nitrogen-doped CDs (NCDs) for our study. A mixture of citric acid and urea was dissolved in 10 mL of deionized water. Then, this solution was sonicated for 10 minutes to completely dissolve citric acid and urea into a colourless solution. The colourless solution was then heated in a domestic microwave for 5 minutes at 800 watts to form a dark-brown, clustered solid, which was then baked for an hour at 60 °C in a preheated oven. After the solution had cooled to room temperature, 20 ml of deionized water was added for dilution to the CDs and NCDs samples and sonicated for 10 minutes. Lastly, another 20 ml of deionized water was added to CDs and NCDs solutions before they were centrifuged at 3000 rpm for 20 minutes to remove large or agglomerated particles. The as-prepared CDs and NCDs solutions were stored at room temperature.

Table 1 Ratio of citric acid and urea

Sample	Product	Citric Acid (g)	Urea (g)
A	CD	3	0
B	NCD1	3	1
C	NCD2	3	2
D	NCD3	3	3

2.3 Characterization and ECL measurement of Carbon Dots and Nitrogen-doped Carbon Dots

The formation of CDs and NCDs was confirmed by Lambda 950 UV-Visible Spectrometer (PerkinElmer). The functional groups on CDs and NCDs were validated by Spectrum 65 FT-IR Spectrometer (PerkinElmer). All electrochemical measurements used a screen-printed electrode (SPE) (EP-P; Biodevice Technology Co. Ltd., Japan). The three-electrode SPE system includes a carbon-based working electrode, a counter electrode, and an Ag/AgCI reference electrode. As depicted in Figure 1, the working electrode surface is 2.64 mm^2, and the overall size of the connection part and the carbon barrier to prevent the solution from flowing to the connector is 12.5 mm × 4 mm x 0.3 mm [18-19]. A 20 µl solution was applied directly onto the three-electrode surface and was discarded after a single use. All ECL measurements were carried out using a USB-powered potentiostat (BDTeCL-XP; Japan's Biodevice Technology Co. Ltd.) and data were collected using the uPMT-STAT V2 software.

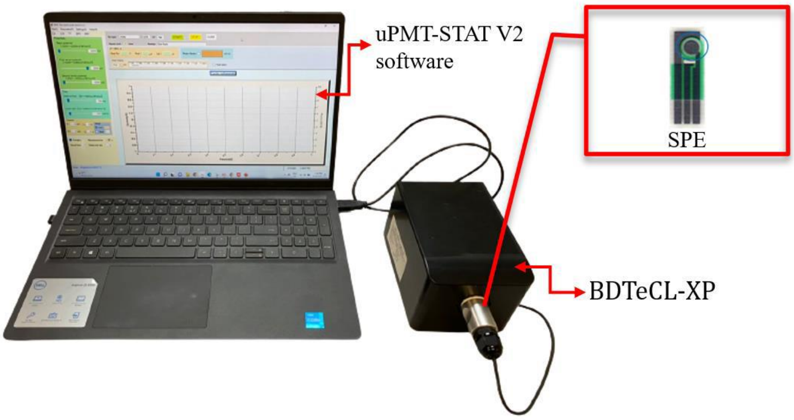

Figure 1. ECL experimental setup.

ECL mechanisms of CDs and NCDs were investigated in various electrolytes, namely PBS (0.1 M PBS, pH 7.4), PBS with 0.1 M KCl, PBS with 0.1 M $K_2S_2O_8$ and PBS with 0.1 M $K_2S_2O_8$ and 0.1 M KCl through cyclic voltammetry (CV) at a potential range of +2 to -2 V and a scan rate of 100 mV/s. Then, NCD3 was selected for studies on the effect of the CV potential range between +2 and -2 V and 0 and -2 V on ECL intensity. Apart from that, the effect of luminophore, supporting electrolyte, and co-reactant concentrations on ECL intensity were conducted in a 30x dilution of as prepared NCD3 in PBS with 0.1 M $K_2S_2O_8$ and 0.1 M KCl at a potential scan of 0 to -2 V and a scan rate of 100 mV/s, except for the optimization of luminophore concentration, where NCD3 was diluted 20x, 30x, 40x, and 50x. Each parameter was repeated three times.

3. RESULTS AND DISCUSSION

3.1 Structures and optical properties of NCDs and CDs

The formation of CDs and NCDs was confirmed by UV-vis absorption spectra. Figure 2(a) shows CD, NCD1, NCD2 and NCD3 exhibit the absorption peak at 237 nm, which is assigned to the typical aromatic $\pi - \pi^*$ transition, confirming the formation of graphitic cores of CDs [20-21]. After urea was added to citric acid to form NCD1, an absorbance peak was observed at 340 nm. The same absorbance peak was also observed for NCD2. However, NCD3 shows two distinct absorbance peaks at 340 and 414 nm. These absorbance peaks represent the $n - \pi^*$ transition, which demonstrates that nitrogen groups are conjugated to the graphitic cores of CDs [17, 22]. As a result, we were able to successfully synthesize CDs using only citric acid and NCDs with the addition of urea through the microwave-assisted method.

FT-IR was used to evaluate the surface functional groups on CDs and NCDs as shown in Figure 2(b). The broad peak centered at 3379 cm^{-1} revealed O-H and N-H bonding [17, 23]. Meanwhile, peaks at 1638 cm^{-1} and 1364 cm^{-1} correspond to the C=O and CH_2 bond, respectively, which are related to the benzene skeletal vibrations of conjugated sp^2 carbon [17]. The absorption peak at 1216 cm^{-1} indicates the C–N amine stretching vibration [15]. As the amount of urea increases from sample NCD1 to NCD3, each absorption peak shows an increase in intensity. As a consequence, it could be concluded that the surfaces of CDs and NCDs are occupied with hydrophilic groups that make them water-soluble. These observations also confirmed that nitrogen was successfully doped into the CDs and that increasing the amount of urea results in an increase in nitrogen concentration on CDs.

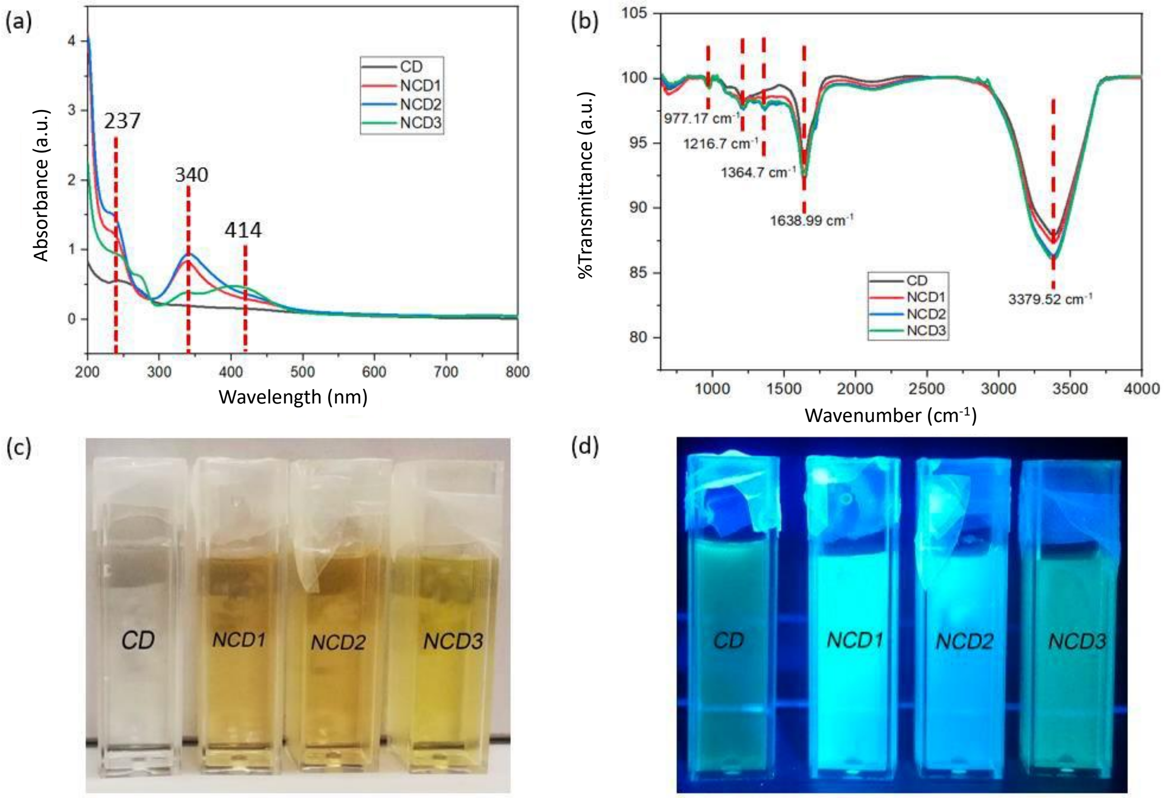

FIGURE 2. (a) UV–vis absorption, (b) FT-IR spectra and photographs of CDs and NCDs under (c) normal and (d) UV light.

A photograph of the aqueous solution of CDs shows almost colorless behavior under ambient light, as shown in Figure 2(c) but emits pale blue fluorescence under a UV lamp with a wavelength of 365 nm, as shown in Figure 2(d). Meanwhile, diluted NCD1, NCD2 and NCD3 show a light brown color under normal light, which could also be easily observed with the naked eye, but emit a bright blue to almost green fluorescence color under a UV lamp. This observation has exhibited that the concentration of nitrogen-doped CDs may tune the fluorescence properties of NCDs [14].

3.2 Electrochemiluminescence of CD, NCD1, NCD2 and NCD3

In order to understand the ECL mechanism of CDs and NCDs on SPE, we performed cyclic voltammetry (CV) in various electrolyte conditions, as depicted in Figure 3. CDs and NCDs were tested in PBS with and without the supporting electrolyte KCl to observe the possibility of an annihilation pathway in the ECL reaction. Meanwhile, the addition of potassium persulfate ($K_2S_2O_8$) in PBS with and without the supporting electrolyte KCl was conducted to verify the co-reactant mechanism in the ECL reaction. During the reverse scan of CV (Figure 3(a)), CDs in PBS with and without KCl show a reduction peaks at -0.78 V, indicating the formation of $CD^{\bullet-}$. This observation can also be seen on NC1, NCD2 and NCD3 at reduction peak of -0.60 V, -0.58 V, and -0.52 V, respectively (Figure 3(b-d)). However, no significant ECL emission is observed in PBS with and without KCl for all CDs and NCDs (Figure 3(e-h)). These results indicate an annihilation reaction does not occur to produce ECL emissions, or the radical cation and radical anion may be formed, but they are not so stable or are short-lived, so the effective electron transfer cannot occur near the working electrode to generate the excited states to produce the obvious photocurrent [24].

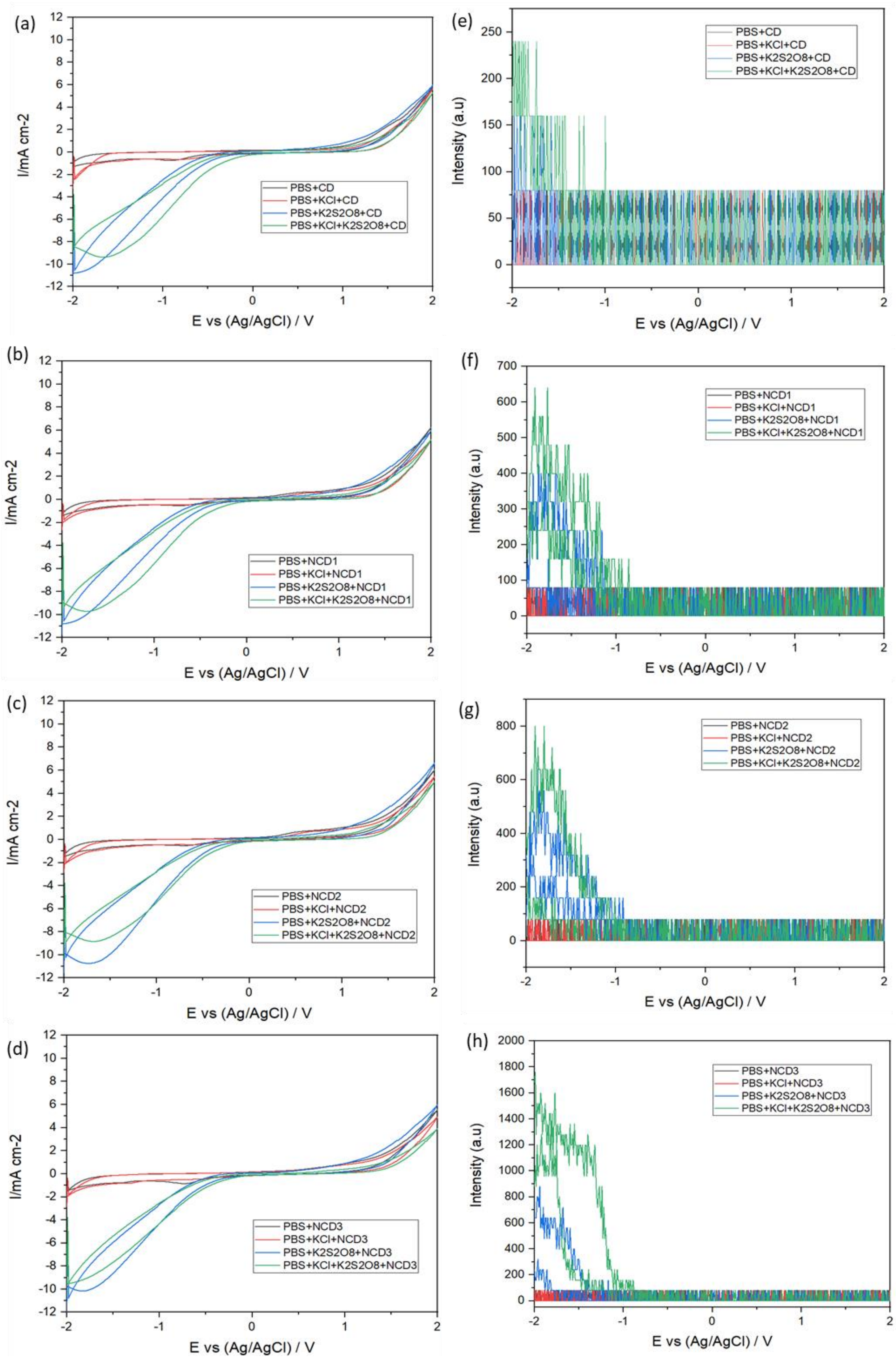
(a)
I/mA cm-2
E vs (Ag/AgCl) / V
PBS+CD
PBS+KCl+CD
PBS+K2S2O8+CD
PBS+KCl+K2S2O8+CD
(e)
Intensity (a.u)
E vs (Ag/AgCl) / V
PBS+CD
PBS+KCl+CD
PBS+K2S2O8+CD
PBS+KCl+K2S2O8+CD
(b)
I/mA cm-2
E vs (Ag/AgCl) / V
PBS+NCD1
PBS+KCl+NCD1
PBS+K2S2O8+NCD1
PBS+KCl+K2S2O8+NCD1
(f)
Intensity (a.u)
E vs (Ag/AgCl) / V
PBS+NCD1
PBS+KCl+NCD1
PBS+K2S2O8+NCD1
PBS+KCl+K2S2O8+NCD1
(c)
I/mA cm-2
E vs (Ag/AgCl) / V
PBS+NCD2
PBS+KCl+NCD2
PBS+K2S2O8+NCD2
PBS+KCl+K2S2O8+NCD2
(g)
Intensity (a.u)
E vs (Ag/AgCl) / V
PBS+NCD2
PBS+KCl+NCD2
PBS+K2S2O8+NCD2
PBS+KCl+K2S2O8+NCD2
(d)
I/mA cm-2
E vs (Ag/AgCl) / V
PBS+NCD3
PBS+KCl+NCD3
PBS+K2S2O8+NCD3
PBS+KCl+K2S2O8+NCD3
(h)
Intensity (a.u)
E vs (Ag/AgCl) / V
PBS+NCD3
PBS+KCl+NCD3
PBS+K2S2O8+NCD3
PBS+KCl+K2S2O8+NCD3

Figure 3. CV (a - d) and ECL intensity (e - h) of CDs and NCDs in PBS buffer (pH 7.4) with or without co-reactant ($K_2S_2O_8$) and supporting electrolyte (KCl).

The reverse scan CV of CDs in PBS with $K_2S_2O_8$ addition (Figure 3(a)) shows a steep onset current reduction beginning at -0.35 V and peaking at -1.80 V. Meanwhile, the same electrolyte with KCl demonstrated reverse onset potential at -0.10 V and a maximum peak at -1.58 V. During this time, both $K_2S_2O_8$ and CDs are electrochemically reduced to $SO_4^{\bullet-}$ and $CD^{\bullet-}$ as per equations (5) and (6). Then, the reaction between $SO_4^{\bullet-}$ and $CD^{\bullet-}$ results in an exited state CD^* that emits a photon in order to return to the ground state via a radiative pathway as per equation (7) and (8). Therefore, ECL emission has been observed in Figure 3(e), starting at an onset potential of -2 V for CDs in PBS with the addition of $K_2S_2O_8$ and -1.85 V for CDs in PBS with the addition of $K_2S_2O_8$ and KCl. This result indicates a co-reactant pathway using $K_2S_2O_8$ is able to produce ECL emissions. Furthermore, supporting electrolyte KCl has improved $SO_4^{\bullet-}$ generation, promoting abundant CD production, as evidenced by the 33.3% increase in ECL intensity recorded.

As for various concentrations of nitrogen-doped CDs, the CV reverse onset potential of NCD1, NCD2 and NCD3 in PBS with the addition of $K_2S_2O_8$ are observed at -0.30 V, -0.23 V and -0.21 V, respectively (Figure 3(b-d)). Meanwhile, the same electrolyte with KCl demonstrated an earlier CV reverse onset potential at -0.21 V, -0.18 V and -0.11 for NCD1, NCD2 and NCD3, respectively. Figure 3(f-h) displays that the ECL emission onset potential begin at -1.97 V, -1.85 V and -1.82 V for NCD1, NCD2 and NCD3, respectively, in PBS with the addition of $K_2S_2O_8$. ECL emission of NCD1, NCD2 and NCD3 in PBS with the addition of $K_2S_2O_8$ and KCl at -1.70 V, -1.68 V and -1.23 V, respectively. This result indicates that KCl has a significant role in facilitating faster ECL reactions in the NCD-$K_2S_2O_8$ co-reactant pathway. Moreover, the ECL intensity of NCD1, NCD2 and NCD3 is significantly increased in PBS with the addition of $K_2S_2O_8$ and KCl electrolytes, indicating that the concentration of nitrogen doped on CDs also plays an important role in the ECL reaction. NCD3 shows the highest ECL intensity by an increment of 86.4% in comparison to CDs in PBS with the addition of $K_2S_2O_8$ and KCl.

3.3 Optimization of Electrochemiluminescence Measurement

NCD3 was selected to run a series of ECL optimizations, namely CV potential range, luminophore, supporting electrolyte, and co-reactant concentrations, as depicted in Figure 4. CV potential range is an important factor due to its effect on electrochemical reactions. Figure 4(a) shows two sets of investigated potential scans, ranging from +2 to -2 V and 0 to -2 V, respectively. The reverse onset potential of CV starting at +2 V and 0 V occurs at -0.25 and -0.3, respectively. The slightly different reverse onset potential does have a great effect on ECL intensity by adding a 52.9% increment for CV starting at +0 V. This could be due to the fact that more NCDs and $K_2S_2O_8$ are effectively reduced electrochemically to form $CD^{\bullet-}$ and $SO_4^{\bullet-}$ between 0 and -2 V in order to produce CD* that emits light at 200 mV earlier ECL onset potential than the +2 to -2 V scan range. As a result, 0 to -2 V is chosen as the optimum CV range potential. This study has shown that as-prepared CDs and NCDs can act as luminophores to produce ECL emission using a co-reactant pathway. However, the as-prepared CDs and NCDs are very concentrated. Therefore, we need to optimize the concentration of luminophore by dilution with PBS, as depicted in Figure 4(b). 20x NCD3 dilution gives the lowest ECL intensity, which might be due to highly concentrated luminophore quenching the ECL emission, while 50x NCD3 dilution might not have enough luminophore for the ECL reaction. 30x and 40x NCD3 dilutions show almost similar ECL intensities. However, a 30x NCD3 dilution is chosen as the optimum luminophore concentration, with a 2% higher ECL intensity.

A supporting electrolyte must have a variety of qualities, including solvent solubility and electrochemical stability [25]. As a consequence, we selected KCl as the supporting electrolyte due to its ionic strength and conductivity. Figure 4(c) shows that decreasing the KCl concentration significantly reduces ECL intensity. This is due to KCl facilitating the formation of NCDs and peroxydisulfate radicals that generate ECL emissions. Herein, we choose 0.1 M KCl as the optimum supporting electrolyte concentration. ECL emission can be generated with a single potential step at the electrode by adding a co-reactant to a solution that contains a luminophore. This study has proven that NCD3 and $K_2S_2O_8$ can produce ECL emissions using a co-reactant pathway. Figure 4(d) shows that the intensity of the ECL decreases rapidly as the concentration of $K_2S_2O_8$ decreases. This is due to the low $K_2S_2O_8$ concentration, which will lead to a low generation of $SO_4^{\bullet-}$ radicals that play an important role in the generation of $CD^{\bullet-}$. Therefore, the optimum co-reactant concentration selected for this study is 0.1 M of $K_2S_2O_8$ as it produces the highest ECL intensity.

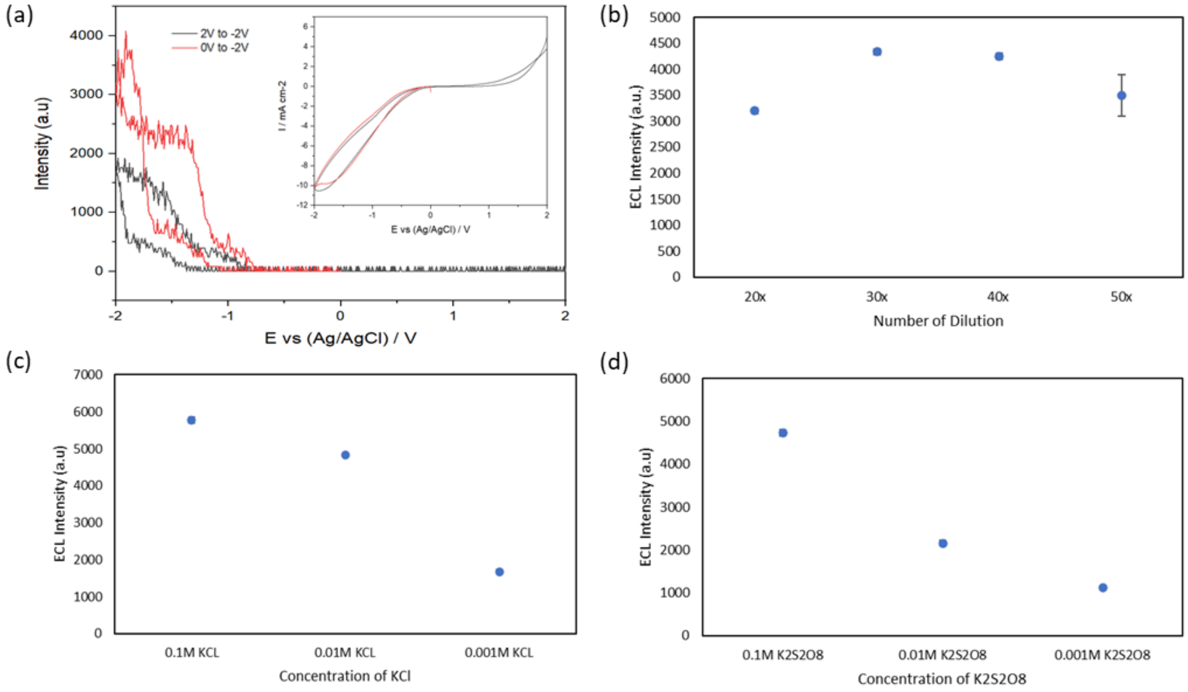

Figure 4. Effect of (a) CV potential range, (b) luminophore, (c) supporting electrolyte and (d) co-reactant concentrations on ECL intensity of NCD3 in 0.1 M PBS.

4. CONCLUSION

In summary, we have synthesized and characterized CDs and NCDs through the microwave-assisted method. These CDs and NCDs have photoluminescence properties that make them suitable as ECL luminophores. The catalytic activity of luminophores (CDs and NCDs) with $K_2S_2O_8$ and KCl as co-reactants and supporting electrolytes has been studied. There is no significant ECL emission observed for all CDs and NCDs in PBS with or without KCl. These results indicate an annihilation reaction does not occur or inefficient electron transfer between short-lived CD's cation and anion radicals to produce ECL emissions. ECL emission has been starting at -1.35 V for CDs in PBS with the addition of $K_2S_2O_8$ and -1.30 V for CDs in PBS with the addition of $K_2S_2O_8$ and KCl. This result indicates a co-reactant pathway using $K_2S_2O_8$ is able to produce ECL emissions. Furthermore, supporting the electrolyte KCl has improved $SO_4^{\bullet-}$ generation, as evidenced by the high ECL intensity recorded. The ECL emission of NCD1, NCD2, and NCD3 in PBS with $K_2S_2O_8$ and KCl addition begins faster, which indicates that KCl has a significant role in facilitating faster ECL reactions in the NCD-$K_2S_2O_8$ co-reactant pathway.

Furthermore, the addition of $K_2S_2O_8$ and KCl electrolytes significantly increases the ECL intensity of NCD1, NCD2, and NCD3 in PBS, indicating that the concentration of nitrogen-doped molecules also plays an important role in the ECL reaction, with NCD3 displaying the highest ECL intensity by 86.4% compared to CDs. The 50 mV difference in CV reverse onset potential shows 52.9% higher ECL intensity for CV starting at 0 V, which could be due to more generations of CDs and peroxydisulfate radicals emitting lights rather than during the potential scan of +2 to -2 V as indicated by the 200 mV early ECL onset potential. $K_2S_2O_8$ and KCl have proven to be good co-reactants and supporting electrolytes for luminophore, especially CDs and NCDs, to produce ECL emission.

ACKNOWLEDGEMENTS

The author would like to acknowledge the support from the Fundamental Research Grant Scheme for Research Acculturation of Early Career Researchers (FRGS-RACER) under a grant number of RACER/1/2019/STG07/UNIMAP//1. A huge appreciation to Prof. Eiichi Tamiya from Osaka University for lending us ECL measurement instrument to carry out this research.

REFERENCES

[1] Lim, S.Y., Shen, W., Gao, Z., Chem. Soc. Rev. vol **44** (2015) pp. 362-381.

[2] Wang, J., Qiu, J., J Mater Sci vol **51** (2016) pp. 4728-4738.

[3] Dhenadhayalan, N., Lin, K., Saleh, T.A., Small vol **16**, issue 1 (2019) pp. 1905767.

[4] Jana, P., Dev, A., Materials Today Communications vol **32** (2022) pp. 104068

[5] Xie, R., Wang, Z., Zhou, W., Liu, Y., Fan, L., Li, Y., Li, X., Anal. Methods vol **8**, issue 20 (2016) pp. 4001-4016.

[6] Zhang, J., Yu, S. H., Materials Today vol **19**, issue 7 (2016) pp. 382-393.

[7] Medeiros, T. V., Manioudakis, J., Noun, F., Macairan, J. R., Victoria, F., Naccache, R., J. Mater. Chem. C vol **7**, issue 24 (2019) pp. 7175-7195.

[8] Nozaki, T., Kakuda, T., Pottathara, Y. B., Kawasaki, H., Photochem Photobiol Sci vol **18**, issue 5 (2019) pp. 1235-1241.

[9] Richter, M. M., Chem. Rev. vol **104**, issue 6 (2004) pp. 3003-3036.

[10] Li, J., Guo, S., Wang, E., RSC Advances vol **2** (2012) pp. 3579-3586.

[11] Dong, Y., Zhou, N., Lin, X., Lin, J., Chi, Y., Chen, G., Chem. Mater. vol **22**, issue 21 (2010) pp. 5895-5899.

[12] Dong, Y., Chen, C., Lin, J., Zhou, N., Chi, Y., Chen, G., Carbon vol **56**, (2013) pp. 12-17.

[13] Gao, S., Chen, Y., Fan, H., Wei, X., Hu, C., Wang, L., Qu, L., J. Mater. Chem. A vol **2**, issue 18 (2014) pp. 6320-6325.

[14] Liang, G. X., Zhao, K. R., He, Y. S., Liu, Z. J., Ye, S. Y., Wang, L., Microchemical Journal vol **171**, (2021) pp. 106787.

[15] Wang, X., Zhang, M., Huo, X., Zhao, W., Kang, B., Xu, J. J., Chen, H., Nanoscale Adv. vol **1**, issue 5 (2019) pp. 1965-1969.

[16] Zhu, H., Wang, X., Li, Y., Wang, Z., Yang, F., Yang, X., Chem. Commun., issue 34 (2009) 5118-5120.

[17] Qu, S., Wang, X., Lu, Q., Liu, X., Wang, L., Angew. Chem. Int. Ed. vol **51**, issue 49 (2012) pp. 12215-12218.

[18] Ismail, N. S., Le, Q. H., Hasan, Q., Yoshikawa, H., Saito, M., Tamiya, E., Electrochimica Acta vol **180**, (2015) pp. 409-418.

[19] "Biodevice technology for printed electrodes for biosensor development" https://biodevicetech.com/ (accessed Aug. 12, 2022).

[20] Lu, Z., Giles, L. W., Teo, B. M., Tabor, R. F., Colloid and Interface Science Communications vol **46**, (2022) pp. 100571.

[21] Lai, Q., Zhu, S., Luo, X., Zou, M., Huang, S., AIP Advances vol **2**, issue 3 (2012) pp. 032146.

[22] Chen, A., Liang, W., Wang, H., Zhuo, Y., Chai, Y., Yuan, R., Anal. Chem. vol **92**, issue 1 (2020) pp. 1397-1385.

[23] Arcudi, F., Dordevic, L., Prato, M., Angew. Chem. Int. Ed. vol **55**, issue 6 (2016) pp. 2147-2152.

[24] Chen, Y., Lin, J., Zhang, R., He, S., Ding, Z., Ding, L., Analyst vol **146** (2021) pp. 5287-5293.

[25] Balbuena, P. B., "Electrolyte Materials – Issues and Challenges" in AIP Conference Proceedings 1597 (2014) pp. 82-97.